Nucleus ^{26}O: A Barely Unbound System beyond the Drip Line

Y. Kondo,[1] T. Nakamura,[1] R. Tanaka,[1] R. Minakata,[1] S. Ogoshi,[1] N. A. Orr,[2] N. L. Achouri,[2] T. Aumann,[3,4] H. Baba,[5] F. Delaunay,[2] P. Doornenbal,[5] N. Fukuda,[5] J. Gibelin,[2] J. W. Hwang,[6] N. Inabe,[5] T. Isobe,[5] D. Kameda,[5] D. Kanno,[1] S. Kim,[6] N. Kobayashi,[1] T. Kobayashi,[7] T. Kubo,[5] S. Leblond,[2] J. Lee,[5] F. M. Marqués,[2] T. Motobayashi,[5] D. Murai,[8] T. Murakami,[9] K. Muto,[7] T. Nakashima,[1] N. Nakatsuka,[9] A. Navin,[10] S. Nishi,[1] H. Otsu,[5] H. Sato,[5] Y. Satou,[6] Y. Shimizu,[5] H. Suzuki,[5] K. Takahashi,[7] H. Takeda,[5] S. Takeuchi,[5] Y. Togano,[4,1] A. G. Tuff,[11] M. Vandebrouck,[12] and K. Yoneda[5]

[1]*Department of Physics, Tokyo Institute of Technology, 2-12-1 O-Okayama, Meguro, Tokyo 152-8551, Japan*
[2]*LPC Caen, ENSICAEN, Université de Caen, CNRS/IN2P3, F-14050 Caen, France*
[3]*Institut für Kernphysik, Technische Universität Darmstadt, D-64289 Darmstadt, Germany*
[4]*ExtreMe Matter Institute EMMI and Research Division, GSI Helmholtzzentrum für Schwerionenforschung GmbH, D-64291 Darmstadt, Germany*
[5]*RIKEN Nishina Center, Hirosawa 2-1, Wako, Saitama 351-0198, Japan*
[6]*Department of Physics and Astronomy, Seoul National University, 599 Gwanak, Seoul 151-742, Republic of Korea*
[7]*Department of Physics, Tohoku University, Miyagi 980-8578, Japan*
[8]*Departiment of Physics, Rikkyo University, Toshima, Tokyo 171-8501, Japan*
[9]*Department of Physics, Kyoto University, Kyoto 606-8502, Japan*
[10]*Grand Accélérateur National d'Ions Lourds (GANIL), CEA/DRF-CNRS/IN2P3, Bvd Henri Becquerel, 14076 Caen, France*
[11]*Department of Physics, University of York, Heslington, York YO10 5DD, United Kingdom*
[12]*Institut de Physique Nucléaire, Université Paris-Sud, IN2P3-CNRS, Université de Paris Sud, F-91406 Orsay, France*

(Received 27 August 2015; published 9 March 2016)

The unbound nucleus ^{26}O has been investigated using invariant-mass spectroscopy following one-proton removal reaction from a ^{27}F beam at 201 MeV/nucleon. The decay products, ^{24}O and two neutrons, were detected in coincidence using the newly commissioned SAMURAI spectrometer at the RIKEN Radioactive Isotope Beam Factory. The ^{26}O ground-state resonance was found to lie only $18 \pm 3(\text{stat}) \pm 4(\text{syst})$ keV above threshold. In addition, a higher lying level, which is most likely the first 2^+ state, was observed for the first time at $1.28^{+0.11}_{-0.08}$ MeV above threshold. Comparison with theoretical predictions suggests that three-nucleon forces, pf-shell intruder configurations, and the continuum are key elements to understanding the structure of the most neutron-rich oxygen isotopes beyond the drip line.

DOI: 10.1103/PhysRevLett.116.102503

How neutron rich can a bound nucleus be? This fundamental question remains to be fully answered as the location of the neutron drip line—the point at which a nucleus is no longer bound—has been established experimentally only up to the element oxygen ($Z = 8$). Theoretically, the drip line cannot be predicted reliably even by the most sophisticated nuclear models owing to the poorly known character of the nuclear interaction and many-body correlations at extreme neutron-proton asymmetry.

The behavior of the neutron drip line in the vicinity of $Z = 8$ is striking: it is known experimentally that the drip line lies at $N = 16$ for carbon, nitrogen, and oxygen while jumping to at least $N = 22$ for fluorine. This sudden change, sometimes referred to as the "oxygen anomaly" [1], has yet to be properly understood. In this context, the nucleus ^{26}O, with two neutrons more than the last bound oxygen isotope—doubly magic ^{24}O [2–4]—is a key element to understanding this behavior. Indeed, most theories predict ^{26}O and/or ^{28}O ($Z = 8$, $N = 20$) to be bound [5–11]. Explanations for this overbinding may include the effects of three-nucleon forces [1] and coupling to the continuum [12]. The binding energy of the ^{26}O ground state and energies of the low-lying levels—in particular the first 2^+ excited state (2^+_1)—are, therefore, expected to provide a stringent test of many-body theories incorporating such effects. In addition, the 2^+_1 excitation energy is also important to examine the influence of the pf shell orbitals and the extent of the $N = 20$ shell gap below the "island of inversion" [5].

The ground state of ^{26}O has recently been found to be barely unbound with respect to two-neutron emission—by 53 keV (1σ upper limit) in an intermediate energy reaction study [13,14] and 120 keV (upper limit with a 95% confidence level) at high energies [15]. The 2^+_1 state has yet, however, to be located. It may be noted that Ref. [15] claimed the existence of a level at 4.2 MeV, which could be a proton-hole state, although the statistics were limited. This Letter reports on a precise determination of the ground-state energy and the first observation of the 2^+_1 state, by means of invariant-mass spectroscopy following one-proton removal from a ^{27}F beam.

Being extremely weakly unbound with respect to two-neutron emission, ^{26}O has also attracted attention as the first candidate for two-neutron radioactivity. Indeed,

recently Kohley *et al.* deduced a rather long half-life, $T_{1/2} = 4.5^{+1.1}_{-1.5}(\text{stat}) \pm 3(\text{syst})$ ps [16], albeit with relatively large uncertainties. Theoretically [17,18], the ^{26}O ground state may be long lived as (1) sequential neutron emission through ^{25}O is energetically forbidden, (2) the decay energy with respect to $^{24}\text{O} + 2n$ is extremely low, and (3) the most likely configuration is a doubly closed ^{24}O core and two $d_{3/2}$ valence neutrons subject to the corresponding centrifugal barrier. Whether ^{26}O is in fact long-lived depends strongly on the decay energy, while, as noted, only an upper limit has been determined so far. The present work will thus provide a strong constraint on the lifetime.

The experiment was carried out at the Radioactive Isotope Beam Factory (RIBF) operated by the RIKEN Nishina Center and the Center for Nuclear Study (CNS), University of Tokyo. A ^{27}F secondary beam was produced by projectile fragmentation of ^{48}Ca (∼140 pnA) at 345 MeV/nucleon using a 20-mm thick beryllium target. The secondary beam was separated and purified using BigRIPS [19,20] operated with an aluminium achromatic degrader of 15-mm median thickness at the first dispersive focal plane. The momentum acceptance of BigRIPS was ±3% and the ^{27}F beam intensity was typically 1.4×10^3 particles per second. The secondary beam was characterized using thin plastic scintillator timing detectors, a multiwire proportional counter and an ionization chamber mounted just upstream of the carbon secondary reaction target (thickness 1.8 g/cm). The impact position on the target and incident angles of the beam particles were determined event by event using two multiwire drift chambers (MWDCs). The beam energy at the target midpoint was 201 MeV/nucleon. Data were also acquired with the target removed in order to ascertain the contribution of background events produced by materials other than the target. The background is subtracted in decay-energy spectra shown later. In addition to the measurements made of ^{26}O with the ^{27}F beam, data were also taken at 201 MeV/nucleon for one-proton removal from a ^{26}F beam leading to ^{25}O—a system which has been studied previously [15,21] and may serve as a reference for the analysis procedures and simulations.

The decay products, ^{24}O and neutron(s), were measured in coincidence using the newly commissioned spectrometer SAMURAI [22]. The large-gap superconducting dipole magnet of SAMURAI, with a central magnetic field of 3 T, provided for the momentum analysis of the charged particles. The dipole gap was kept under vacuum using a chamber equipped with thin exit windows [23] so as to reduce to a minimum the amount of material encountered by both the fragments and neutrons. The trajectories of the charged fragments were determined using two MWDCs placed at the entrance and exit of the magnet, while a 16 element plastic scintillator hodoscope provided for energy-loss and time-of-flight measurements. The beam velocity

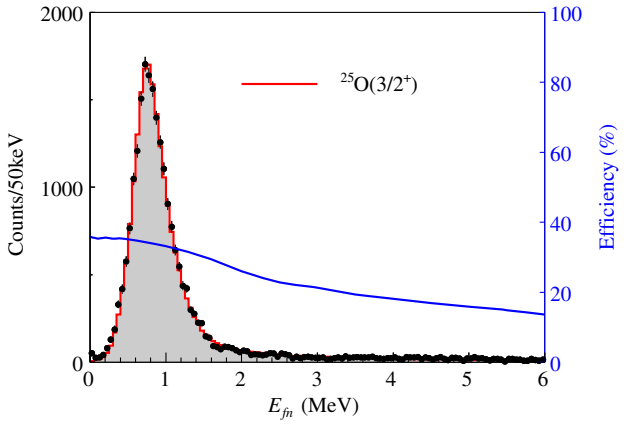

FIG. 1. Decay-energy spectrum of $^{24}\text{O} + n$ observed in one-proton removal from ^{26}F. The red-shaded histogram shows the fit, after accounting for the experimental response of the setup, assuming population of the ground state of ^{25}O. The blue curve represents the overall detection efficiency.

neutrons were detected using the large-acceptance plastic scintillator array NEBULA [22,24], placed some 11 m downstream of the target. The array consists of 120 individual detector modules (each 12 cm × 12 cm × 180 cm) and 24 charged particle veto detectors (thickness 1 cm), arranged in a two-wall configuration, with an interwall separation of 85 cm.

Turning now to the results obtained for ^{25}O, Fig. 1 displays the two-body decay energy E_{fn} for $^{24}\text{O} + n$ reconstructed from the momentum vectors of the fragment and neutron. The known $3/2^+$ ground-state resonance of ^{25}O [15,21] is clearly seen. The resonance energy and width were deduced by fitting the spectrum with a d-wave Breit-Wigner line shape, following the prescription of Ref. [15], after taking into account the experimental response function. In practice this was done using a complete simulation of the setup based on GEANT4 [25] and employing the QGSP_INCLXX physics model for the neutron interactions in NEBULA. The latter was adopted as it reproduces well the single-neutron detection efficiency and crosstalk characteristics of NEBULA which were determined during a dedicated commissioning run with the well-known $^7\text{Li}(p,n)^7\text{Be}(\text{g.s.} + 0.43\ \text{MeV})$ reaction at 200 MeV [24]. The simulation included all experimental effects as well as the beam characteristics and the reaction kinematics. The decay-energy resolution (FWHM) was determined to be 430 keV at $E_{fn} = 750$ keV. A resonance energy of 749(10) keV and width of 88(6) keV were deduced, where the errors quoted include both the statistical and systematic uncertainties. The precision, in particular for the width, has been considerably improved compared to the previous measurements [15,21], owing to the increased statistical quality of the present data. The resonance energy obtained here is consistent with the earlier measurements (725^{+54}_{-29} keV [15] and 770^{+20}_{-10} keV [21]), while the width is in agreement [26] with that of

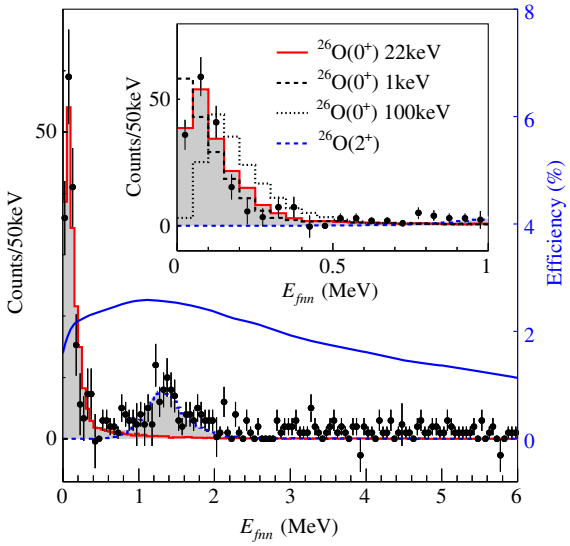

FIG. 2. Decay-energy spectrum, after background subtraction, of ^{26}O reconstructed from the momentum vectors of the in-flight decay products, ^{24}O and two neutrons, from one-proton removal from ^{27}F. The red-solid and blue-dashed histograms represent the best fits (including the experimental response of the setup) to the ground and excited states, with the sum of the two shown by the shaded histogram. The blue curve represents the overall detection efficiency including the crosstalk rejection procedures (see text). The inset shows the near threshold region in detail where, in addition to the best fit result, the simulated experimental responses for ground state decay energies of 1 keV (black-dashed) and 100 keV (black-dotted histogram) are also shown to demonstrate the sensitivity of the present measurements.

Ref. [15] (20^{+60}_{-20} keV) within 2σ. Compared to theory, the present width is close to the 63 keV calculated within the continuum shell model [27] and is also consistent with the single-particle width for d-wave neutron decay [15,21].

Turning now to ^{26}O, Fig. 2 displays the three-body decay energy (E_{fnn}) spectrum reconstructed from the ^{24}O and two neutrons following proton removal from ^{27}F. Importantly, events arising from crosstalk have been eliminated using a causality condition based on the apparent neutron velocity between events registered in NEBULA [24]. Moreover, only events involving the detection of a neutron in the first wall and another in the second wall were retained for analysis so as to reduce the contribution of crosstalk to negligible levels. The crosstalk rejection procedures were adapted from those developed at lower energies [28–30] and the details of the methods used here are described in Ref. [24]. In addition to the ground-state resonance just above threshold, an excited state—most likely the first 2^+ state—is clearly observed for the first time at around 1.3 MeV. On the other hand, no resonance like structure is observed at higher energies as reported in Ref. [15].

The resonance energies of the two states were determined by fitting the ^{26}O decay energy E_{fnn} spectrum with response functions obtained by the full GEANT4 based simulation including the crosstalk rejection procedures. In the simulations, phase space decay with zero lifetime for the ground state was assumed as a first step. For the excited state, sequential decay via the ^{25}O ground state was assumed. This assumption was confirmed by analyzing the E_{fn} spectrum of the binary sub-system $^{24}\mathrm{O}+n$ for the excited state events. The amplitudes and positions of each peak were free fit parameters while the widths of both resonances were set to zero as the apparent widths were entirely dominated by the experimental resolution (FWHM$\simeq$ 110 keV at 20 keV and FWHM $\simeq$ 540 keV at 1.3 MeV). The energies of the ground and excited states determined in this manner were 22^{+14}_{-11} keV and $1.28^{+0.11}_{-0.08}$ MeV, respectively.

As noted in Ref. [15], the ground-state energy may be more precisely determined by analyzing the $^{24}\mathrm{O}+n$ decay-energy spectrum for events [31] arising from the ^{27}F beam (Fig. 3). More specifically, the E_{fn} distribution in the three-body decay is well correlated to the E_{fnn} spectrum since $E_{fnn} \simeq 2\langle E_{fn}\rangle$ irrespective of the decay mode (see below). It may also be noted that the analysis of $^{24}\mathrm{O}+n$ coincidence events has the advantage of providing a much richer data set: some 40 times more events compared to the $^{24}\mathrm{O}+2n$ data set. The peak near $E_{fn}=0$ in the spectrum corresponds to the ^{26}O ground state decay, while the broader structure at about 0.7 MeV arises from the decays of the ^{26}O excited state and the $^{25}\mathrm{O}(3/2^+)$ ground state directly populated from ^{27}F. In the fitting, the energies and widths of the ^{26}O excited state and the $^{25}\mathrm{O}(3/2^+)$ state were fixed to the values determined above. In this manner a ^{26}O ground-state energy of 18(3) keV was deduced, where only the statistical uncertainty is quoted. This result is consistent with that derived from the E_{fnn} analysis but with a significantly reduced uncertainty.

The effects of three-body decay modes other than phase space decay of the ^{26}O ground state have also been examined. Three-body models [17,32] predict an enhancement of "back-to-back" neutron emission in the center of mass, which may be interpreted as a manifestation of the neutron-neutron correlations [32]. Such a decay mode, when incorporated in our simulations, results in a best fit for the ground state resonance energy of 19(3) keV. If, instead, we assume decay whereby the relative decay energy between the neutrons is zero, a resonance energy of 17(3) keV is deduced. These results demonstrate that the ground-state energy is rather model independent. The effect of a possible long half-life on the determination of the ground-state energy was also investigated. Taking, for example, $T_{1/2}=4.5$ ps [16], the fitting of the E_{fn} spectrum provides a value of 19^{+3}_{-4} keV, which is consistent with that obtained assuming no lifetime. Systematic errors other than that associated with the decay mode also arise, principally from the neutron and ^{24}O velocity calibrations and uncertainty in the experimental resolution (mainly from the timing resolution of NEBULA). These two effects are estimated to generate uncertainties of 2 and 3 keV, respectively. Combining the systematic errors (quadratic sum), we adopt $18 \pm 3(\mathrm{stat}) \pm 4(\mathrm{syst})$ keV as the

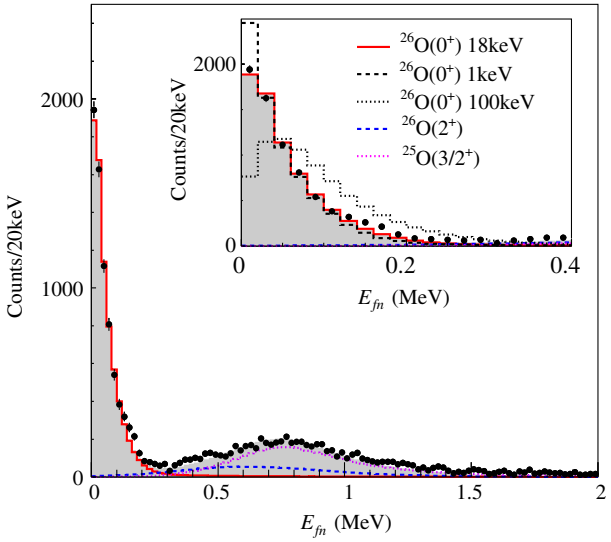

FIG. 3. Decay-energy spectrum of $^{24}\mathrm{O}+n$ arising from the breakup of ^{27}F. The red-solid, blue-dashed, and purple-dotted histograms represent the results of the best-fit simulations for the ^{26}O ground and excited states, and the ^{25}O ground state, respectively. The shaded histogram represents the sum of all three components. The inset shows the near threshold region in detail where, in addition to the best fit result, the simulated experimental responses for ground state decay energies of 1 keV (black-dashed) and 100 keV (black-dotted histogram) are also shown to demonstrate the sensitivity of the present measurements.

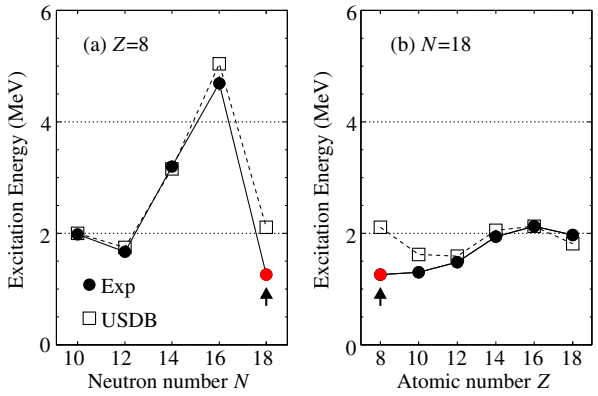

FIG. 4. Experimental 2_1^+ energies (solid circles) for (a) the oxygen isotopes and (b) the $N=18$ isotones together with shell model calculations (open squares) employing the USDB interaction [33]. The present result is denoted by the red filled circle with an arrow.

^{26}O ground state decay energy. We note that the systematic error associated with the ^{26}O excited state decay energy is negligibly small, compared with the statistical one.

The ground-state energy derived here puts a constraint on the lifetime. According to the three-body model of Grigorenko *et al.* [17], an upper limit of 1 keV on the ground-state energy may be deduced from the half-life deduced by Kohley *et al.* [16], which is inconsistent with the result presented here. Based on the relation between the decay energy and lifetime predicted by the three-body model, the decay energy deduced here of 18 keV corresponds to a half-life of the order of $T_{1/2}\sim 10^{-17}-10^{-15}$ s. It should be noted, however, that this estimate is rather model dependent. As such, further measurements to constrain the lifetime are to be encouraged.

The energy of the excited state of ^{26}O is compared with that of the 2_1^+ states of other oxygen isotopes and of the $N=18$ isotones in Fig. 4 together with shell model calculation using the USDB effective interaction [33], which reproduces well the properties of *sd*-shell nuclei. The 2_1^+ excitation energy determined here for ^{26}O is much lower than the 4.7 MeV [3,4] of ^{24}O, confirming the $N=16$ subshell closure at ^{24}O. The USDB calculations reproduce well the trend for the oxygen isotopes, although the energy predicted for ^{26}O is somewhat higher (~800 keV) than observed here. The character of this discrepancy is more evident in Fig. 4(b), whereby difference between the experimental and shell-model energies increase as Z decreases from 12 to 8. Such a behavior indicates the importance of effects which are not incorporated in the USDB interaction.

The structure of ^{26}O may be influenced by shell evolution, *nn* correlations, and continuum effects. The relevance of three-nucleon forces was also suggested [1]. Figure 5 provides a comparison of the presently determined 2_1^+ energy with a range of calculations [33–38]. In terms of shell evolution, intruder *pf* configuration may play a role as the USDB calculation is limited to the *sd* shell model space and cannot properly describe adjacent nuclei in the island of inversion (see, e.g., Fig. 10 of Ref. [33]). Such a conjecture is in line with recent theoretical work whereby an extended model space was found to be important to describe the level schemes of the neutron-rich oxygen isotopes [39]. The effects of *nn* correlation have been discussed in the context of three-body models [34,35] under the assumption of an inert ^{24}O core. The work of Ref. [34] shows that the *nn* interaction is important in reproducing the very low decay energy of the ground state while it is less sensitive to the 2_1^+ decay energy. Continuum effects have been incorporated in shell model calculations [36,37] based on well-studied phenomenological effective interactions. In Ref. [37], the effect of continuum coupling on level energies in very neutron-rich oxygen isotopes is evaluated to be more than 1 MeV. In terms of three-nucleon forces, the pioneering work by Otsuka *et al.* pointed out the significance in the binding of neutron-rich oxygen isotopes [1]. The result of an *ab initio* shell model calculation [38] based on chiral nucleon-nucleon and three-nucleon interactions, where continuum effects are not included, is also shown in Fig. 5. Such results are promising, however, in order to pin down the various effects quantitatively, further developments are required. Experimentally, the next step will be to attempt to access ^{28}O ($Z=8$, $N=20$), which should provide an even more stringent test of the models.

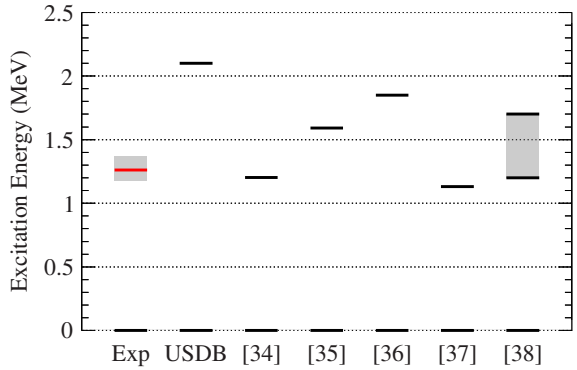

FIG. 5. Comparison of the 2_1^+ energy measured here (red) with theoretical calculations. The experimental uncertainty is represented by the shading. The shaded area of Ref. [38] indicates the uncertainties associated with the modeling.

Finally, it is worth noting that ^{26}O is a unique three-body quantum system in which the ground state can decay only by two-neutron emission with an energy of less than 20 keV (the smallest known to date). In this context, the prediction of the three-body model [32], noted above, that spatial two-neutron correlations are reflected by enhanced "back-to-back" neutron emission deserves special attention in future studies.

In conclusion, invariant mass spectroscopy of the unbound nucleus ^{26}O has been performed following one-proton removal from ^{27}F. The ground state was found to lie only $18 \pm 3(\text{stat}) \pm 4(\text{syst})$ keV above the two-neutron decay threshold. Such an energy favors a half-life much shorter than that recently reported [16]. In addition to the ground state, the first 2^+ state was observed for the first time at $1.28^{+0.11}_{-0.08}$ MeV above threshold. A remeasurement of ^{25}O in proton removal from a ^{26}F beam allowed the ground state energy 749(10) keV and width 88(6) keV to be determined with improved precision with respect to earlier works [15,21].

Comparison of the $^{26}\text{O}(2_1^+)$ energy with theory suggests that three-nucleon forces, pf-shell intruder configurations, as well as a proper treatment of the continuum are key elements to understanding the structure of the heaviest oxygen isotopes. Further theoretical developments along these lines, together with the mapping to higher mass of the neutron drip line, as well as the spectroscopy of the associated unbound systems are clearly desirable next steps in understanding the limits of stability. In this context, the present results demonstrate the power of the SAMURAI setup combined with the intense radioactive beams of very neutron-rich nuclei available at the RIBF-RIKEN.

We wish to extend our thanks to the accelerator staff of the RIKEN Nishina Center for their efforts in delivering the intense ^{48}Ca beam. The present work was supported in part by JSPS KAKENHI Grant No. 24740154, MEXT KAKENHI Grant No. 24105005, the WCU (R32-2008-000-10155-0) and the GPF (NRF-2011-0006492) programs of NRF Korea, and the HIC for FAIR. N. L. A., F. D., J. G., F. M. M., and N. A. O. acknowledge partial support from the Franco-Japanese LIA-International Associated Laboratory for Nuclear Structure Problems. A. N. would like to acknowledge the JSPS Invitation fellowship program for long term research in Japan at the Tokyo Institute of Technology.

[1] T. Otsuka, T. Suzuki, J. D. Holt, A. Schwenk, and Y. Akaishi, Phys. Rev. Lett. **105**, 032501 (2010).
[2] A. Ozawa, T. Kobayashi, T. Suzuki, K. Yoshida, and I. Tanihata, Phys. Rev. Lett. **84**, 5493 (2000).
[3] C. R. Hoffman *et al.*, Phys. Lett. B **672**, 17 (2009).
[4] K. Tshoo *et al.*, Phys. Rev. Lett. **109**, 022501 (2012).
[5] E. K. Warburton, J. A. Becker, and B. A. Brown, Phys. Rev. C **41**, 1147 (1990).
[6] A. Poves, J. Retamosa, M. J. G. Borge, and O. Tengblad, Z. Phys. A **347**, 227 (1994).
[7] Z. Ren, W. Mittig, B. Chen, and Z. Ma, Phys. Rev. C **52**, R20 (1995).
[8] H. Masui, K. Katō, and K. Ikeda, Eur. Phys. J. A **42**, 535 (2009).
[9] A. Shukla, S. Åberg, and S. K. Patra, J. Phys. G **38**, 095103 (2011).
[10] P. Möller, J. R. Nix, and K.-L. Kratz, At. Data Nucl. Data Tables **66**, 131 (1997).
[11] H. Koura, Prog. Theor. Exp. Phys. **2014**, 113D02 (2014).
[12] G. Hagen, M. Hjorth-Jensen, G. R. Jansen, R. Machleidt, and T. Papenbrock, Phys. Rev. Lett. **108**, 242501 (2012).
[13] Z. Kohley *et al.*, Phys. Rev. C **91**, 034323 (2015).
[14] E. Lunderberg *et al.*, Phys. Rev. Lett. **108**, 142503 (2012).
[15] C. Caesar *et al.*, Phys. Rev. C **88**, 034313 (2013).
[16] Z. Kohley *et al.*, Phys. Rev. Lett. **110**, 152501 (2013).
[17] L. V. Grigorenko, I. G. Mukha, and M. V. Zhukov, Phys. Rev. Lett. **111**, 042501 (2013).
[18] L. V. Grigorenko, I. G. Mukha, C. Scheidenberger, and M. V. Zhukov, Phys. Rev. C **84**, 021303 (2011).
[19] T. Kubo, Nucl. Instrum. Methods Phys. Res., Sect. B **204**, 97 (2003).
[20] T. Ohnishi *et al.*, J. Phys. Soc. Jpn. **79**, 073201 (2010).
[21] C. R. Hoffman *et al.*, Phys. Rev. Lett. **100**, 152502 (2008).
[22] T. Kobayashi *et al.*, Nucl. Instrum. Methods Phys. Res., Sect. B **317**, 294 (2013).
[23] Y. Shimizu, H. Otsu, T. Kobayashi, T. Kubo, T. Motobayashi, H. Sato, and K. Yoneda, Nucl. Instrum. Methods Phys. Res., Sect. B **317**, 739 (2013).
[24] T. Nakamura and Y. Kondo, arXiv:1512.08380.
[25] S. Agostinelli *et al.*, Nucl. Instrum. Methods Phys. Res., Sect. A **506**, 250 (2003).
[26] Direct comparison with the result of Ref. [21] is not possible, as a somewhat different formulation was employed for the line shape.
[27] A. Volya and V. Zelevinsky, Phys. At. Nucl. **77**, 969 (2014).
[28] T. Nakamura *et al.*, Phys. Rev. Lett. **96**, 252502 (2006).
[29] J. Wang, A. Galonsky, J. J. Kruse, P. D. Zecher, F. Deák, Á Horváth, Á Kiss, Z. Seres, K. Ieki, and Y. Iwata, Nucl. Instrum. Methods Phys. Res., Sect. A **397**, 380 (1997).

[30] F. M. Marqués, M. Labiche, N. A. Orr, F. Sarazin, and J. C. Angélique, Nucl. Instrum. Methods Phys. Res., Sect. A **450**, 109 (2000).
[31] For events with a neutron multiplicity greater than one, the signal with the shortest TOF was retained.
[32] K. Hagino and H. Sagawa, Phys. Rev. C **89**, 014331 (2014).
[33] B. A. Brown and W. A. Richter, Phys. Rev. C **74**, 034315 (2006).
[34] K. Hagino and H. Sagawa, Phys. Rev. C **90**, 027303 (2014).
[35] L. V. Grigorenko and M. V. Zhukov, Phys. Rev. C **91**, 064617 (2015).
[36] A. Volya and V. Zelevinsky, Phys. Rev. C **74**, 064314 (2006).
[37] K. Tsukiyama, T. Otsuka, and R. Fujimoto, Prog. Theor. Exp. Phys. **2015**, 093D01 (2015).
[38] S. K. Bogner, H. Hergert, J. D. Holt, A. Schwenk, S. Binder, A. Calci, J. Langhammer, and R. Roth, Phys. Rev. Lett. **113**, 142501 (2014).
[39] J. D. Holt, J. Menéndez, and A. Schwenk, Eur. Phys. J. A **49**, 39 (2013).